Lithuanian Journal of Physics
Vol. **66**, No. 1, pp. 61–68 (2026)
ISSN 1648-8504 eISSN 2424-3647
DOI: https://doi.org/10.3952/physics.2026.66.1.7

ON THE PROTON SPIN DIFFUSION IN POWDERED FUMARIC ACID

L. Dagys

Institute of Chemical Physics, Faculty of Physics, Vilnius University, Saulėtekio 3, 10257 Vilnius, Lithuania
Email: laurynas.dagys@ff.vu.lt

Received 1 December 2025; accepted 21 January 2026

Spin diffusion is a well-established phenomenon in solid-state NMR, providing means to probe the molecular structure and transfer magnetization over extended intramolecular distances. Recently, we demonstrated that highly polarized ^{13}C nuclei in 1-^{13}C-fumaric acid can relay magnetization across crystallite boundaries to other ^{13}C-labelled powders. To explore the possibility of using the abundant ^{1}H network, in the present study, dry powdered fumaric acid was examined using conventional solid-state NMR techniques characterizing local order, relaxation and dynamical properties. The results reveal that, although ^{1}H spin diffusion is intrinsically slow, both the diffusion rate and polarization lifetime increase with temperature. This offers new practical insights into the proton-mediated spin diffusion and may aid in designing more efficient polarization-relay strategies.

Keywords: solid-state NMR, spin diffusion, cross-polarization

1. Introduction

Nuclear magnetic resonance (NMR) spectroscopy offers an exceptional control over nuclear spin systems, enabling the observation, manipulation and redirection of magnetization dynamics with a high precision. This ability to probe spin dynamics under a variety of experimental conditions makes NMR an indispensable tool for exploring molecular structure in the solid state. Among the many spin-based processes accessible to NMR, spin diffusion remains one of the most extensively studied, as it provides insight into both the local and long-range organization of nuclear spins [1–17].

Spin diffusion describes the spontaneous or driven transport of nuclear magnetization through dipole–dipole couplings within a spin network. This process spreads magnetization gradients across the lattice via mutual spin flips, allowing structural information to be obtained on the nanometre scale without requiring the long-range order in the sample [1–7]. Spin diffusion also plays a central role in solid-state NMR studies of soft and heterogeneous materials, where it is used to probe intermolecular contacts, measure domain sizes, and characterize structural heterogeneity [1, 3, 4, 6]. The process is also gaining more attention as a means of transporting polarization to other target analytes. In particular, in hyperpolarization methods based on dynamic nuclear polarization (DNP), spin diffusion mediates the propagation of hyperpolarization from the initially polarized sites to surrounding nuclear spins enabling a good general strategy for polarization distribution [8–10].

In our previous work, we also demonstrated that ^{13}C spin polarization can be relayed even across individual crystallites from precipitated 1-^{13}C-fumaric acid, highlighting the potential of spin diffusion as a mechanism for long-range polarization transfer in solids [11]. However, while ^{13}C spins provide a good spectral separation and long relaxation times, ^{1}H spins possess a higher gyromagnetic ratio and could, in principle, facilitate even more efficient polarization transfer across crystallite boundaries. To evaluate the practicality of such a strategy, it is therefore valuable to first understand the crystal structure and the underlying proton dynamics in the pure, unmodified compound.

In this study, conventional solid-state NMR techniques were employed to characterize ^{1}H spin-diffusion dynamics in dry powdered fumaric acid. By analyzing magnetization exchange over short and long mixing times, the efficiency and temperature dependence of polarization transfer within the proton network was assessed. Results indicate that despite weaker dipolar coupling network in fumaric acid, the increase of temperature can considerably contribute to the diffusion rate and overall polarization lifetime. These findings provide a concise yet informative view of the mechanisms that govern proton-driven spin diffusion and lay the groundwork for optimizing polarization-relay strategies in solid-state systems.

2. Materials and methods

Fumaric acid (CAS: 110-17-8) (powder) was purchased from *Sigma-Aldrich*, ground and packed into a 4 mm zirconia MAS rotor. No other preparation step was applied.

Nuclear magnetic resonance (NMR) experiments were performed on a 400 MHz *Bruker* Avance IIIHD spectrometer using a double resonance 4 mm cross-polarization magic-angle-spinning (CP-MAS) probe. Experiments were performed at a 9.4 T magnetic field generated by *Bruker* Ascend superconducting magnet. Temperature was varied from 300 to 350 K in increments of 10 K using dry nitrogen gas.

For all experiments, ^{1}H hard pulses were set at 70 kHz amplitude, while ^{13}C pulses were set at 66 kHz unless stated otherwise. ^{1}H spectra were acquired with a spectral width of 100 kHz and 4096 data points, while ^{13}C spectra were collected with a 30 kHz spectral width and 2416 data points. An exponential line broadening of 40 Hz was applied to all spectra prior to Fourier transformation.

^{11}H → ^{13}C CP-MAS experiments were performed at a MAS rate of 12 kHz to estimate heteronuclear dipole–dipole interactions at room temperature. Rectangular contact pulses with amplitudes of 58 and 70 kHz were applied on ^{1}H and ^{13}C channels, respectively, satisfying the $n = -1$ Hartmann–Hahn condition. CP build-up curves were averaged over four scans and consisted of 110 points, with contact durations incremented in 20 μs steps from 20 μs to 2.2 ms. Oscillatory CP dynamics were extracted from the fitted CP kinetics using the modified I–I*–S model. After applying 200 Hz line broadening and additional zero-filling, CP frequency profiles were obtained via a two-sided Fourier transform. Detailed descriptions of this procedure can be found in the literature [18–20].

^{1}H longitudinal relaxation times (T_1) were measured using a saturation-recovery pulse sequence consisting of a 20-pulse saturation train and ten variable relaxation delays. ^{13}C T_1 values were determined using an initial ramped ^{1}H → ^{13}C CP step followed by an inversion-recovery sequence with ten variable relaxation delays. The overall relaxation delay for both measurements sets was adjusted according to the estimated ^{1}H T_1 value.

^{1}H spin-diffusion experiments were conducted using the Goldman–Shen pulse sequence [12, 13]. The first delay was fixed at 203 μs to achieve magnetization inversion between two ^{1}H peaks, followed by a variable mixing delay to monitor spin-diffusion kinetics. Room-temperature measurements employed a 100-point dataset with mixing times (τ_m) ranging from 10 μs to 10 ms and from 10 μs to 10 s. Variable-temperature experiments were recorded with 51 points across a 10 μs–10 s mixing-time range. Differential peak integrals were calculated as the normalized difference between the two ^{1}H lineshape integrals. Spin-diffusion times (T_{SD}) and rates (R_{SD}) were obtained by nonlinear least-squares fitting to a monoexponential decay function.

All relaxation and ^{1}H spin-diffusion experiments were performed at a MAS rate of 14 kHz to improve proton spectral resolution.

3. Results and discussion

3.1. Fumaric acid structure

The highly symmetric fumaric acid crystal yields well-resolved ^{1}H and ^{13}C MAS NMR spectra, as shown in Fig. 1. Since the largest ^{1}H–^{1}H homonuclear dipolar coupling in the structure does not exceed 5.1 kHz, a MAS frequency above 10 kHz is sufficient to obtain fully resolved isotropic chemical shifts, as clearly evident in the spectra. Nevertheless, minor differences are observed in the ^{1}H lineshapes. The carboxylic proton resonance is approximately 100 Hz broader than the alkene proton resonance and exhibits a lower signal intensity. This difference likely arises from the larger chemical-shift anisotropy (CSA) of the hydroxyl (OH) proton compared to the alkene (CH) protons and is consistent

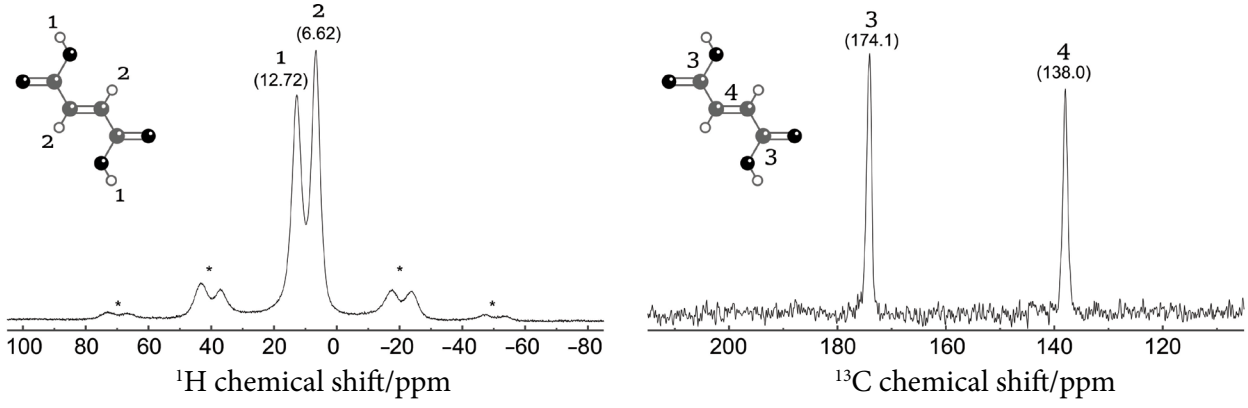

Fig. 1. NMR spectra of fumaric acid recorded under 12 kHz MAS. ^{1}H Bloch decay spectrum (left), ^{1}H → ^{13}C cross-polarized ^{13}C spectrum (right) acquired using 1 ms linearly ramped (from 0 to 70 kHz in amplitude) ^{1}H contact pulse during a rectangular 70 kHz ^{13}C pulse. Numbers indicate ^{1}H and ^{13}C nuclear sites with a chemical shift written in brackets. Asterisks mark MAS spinning sidebands.

with previous reports on other carboxylic acids [21, 22]. In contrast, no corresponding linewidth variation is detected in the ^{13}C spectrum and therefore the intensity difference between the two ^{13}C signals is attributed to variations in cross-polarization (CP) build-up kinetics rather than to CSA differences.

Further structural insights into fumaric acid were obtained from the CP frequency profiles shown in Fig. 2. Profiles were processed following the procedure detailed in Refs. [19, 20]. The procedure starts by fitting the modified I–I*–S CP model that captures the dynamics in the bulk. Later, this is used to extract only the local oscillatory part of CP, which is then used to determine the heteronuclear dipole coupling. CP profiles reveal two distinct types of heteronuclear dipole–dipole interactions corresponding to the carboxylic and alkene functional groups. Moreover, the CH pair displays several well-resolved MAS sidebands in the CP profile. Such sidebands typically arise when the abundant ^{1}H spin network is relatively weak compared to the heteronuclear coupling. Under these conditions, instead of efficiently equilibrating with the ^{1}H spin bath, the system reaches a quasi-equilibrium state that is synchronized with the sample rotation [23].

The dipolar coupling constant for the CH pair was determined by multiplying the observed spectral splitting in Fig. 2 by $\sqrt{2}$ to account for

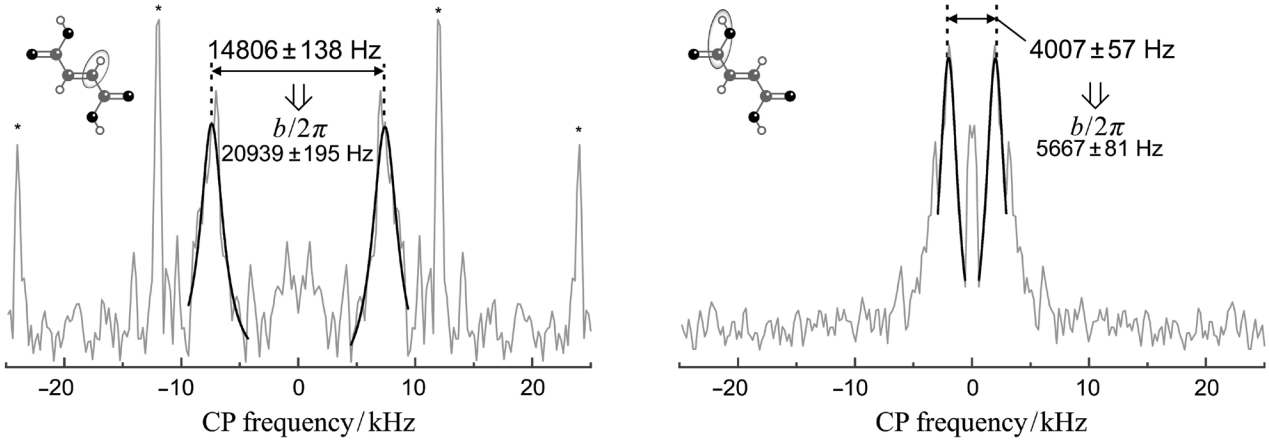

Fig. 2. ^{1}H → ^{13}C cross-polarization (CP) build-up frequency profile acquired using n = –1 Hartmann–Hahn matching condition for alkene (left) and carboxyl (right) ^{13}C heteronuclear pairs. Profiles were acquired following the processing protocol described in Refs. [18–20]. The frequency separation of the Voigt-fitted peaks (black lines) and the associated dipolar coupling constants are given above. Asterisks mark periodic CP quasi-equilibriums which match MAS frequency (12 kHz). Experimental details are given in the text.

the $n = -1$ Hartmann–Hahn matching condition [24–26]. The resulting value of approximately 21 kHz is consistent with the expected value of 23 kHz for a rigid CH bond with an internuclear distance of 1.09–1.10 Å. Moreover, the ratio between the experimentally measured dipolar coupling constant and that of the rigid crystal enables the determination of the local order parameter *S*, which in this case is 0.91, indicative of a highly rigid bond [19, 27, 28]. Similarly, a dipolar coupling of 5.7 kHz for the carboxylic pair corresponds to an internuclear distance of 1.75 Å, in excellent agreement with crystallographic data [29]. Together, these findings confirm the generally high intramolecular rigidity within the crystal lattice of fumaric acid, while the homonuclear dipole–dipole interactions remain comparatively weak due to a large proton separation.

3.2. Spin diffusion kinetics

The strength of spin communication between homonuclear sites in the ^{1}H network was additionally evaluated using the Goldman–Shen pulse sequence, illustrated in Fig. 3(a). The initial delay was adjusted to achieve selective inversion between two proton sites, thereby maximizing the polarization difference, while the subsequent delay monitored the equilibration process (Fig. 3(b)). Equilibration was quantified by calculating the relative difference in integrated signal intensities, which gradually decreases and vanishes due to spin diffusion, as shown in Fig. 3(c). The longitudinal ^{1}H relaxation times were found to be significantly longer (exceeding 168 s) and were therefore neglected in the analysis.

Both short- and long-mixing-time dynamics were investigated. The long mixing times, ranging from 10 μs to 10 s, revealed slow equilibration processes (Fig. 3(c)). Although several spin-diffusion models have been proposed, the data were best described by a monoexponential decay, providing a suitable fit ($R^2 = 0.996$), suggestive of homogeneous long-range dynamics. A similar behaviour has previously been observed and modelled in single-crystal lattices between spectrally-resolved spin species [6, 7]. It is therefore hypothesized that, as the applied MAS frequency exceeds the strongest

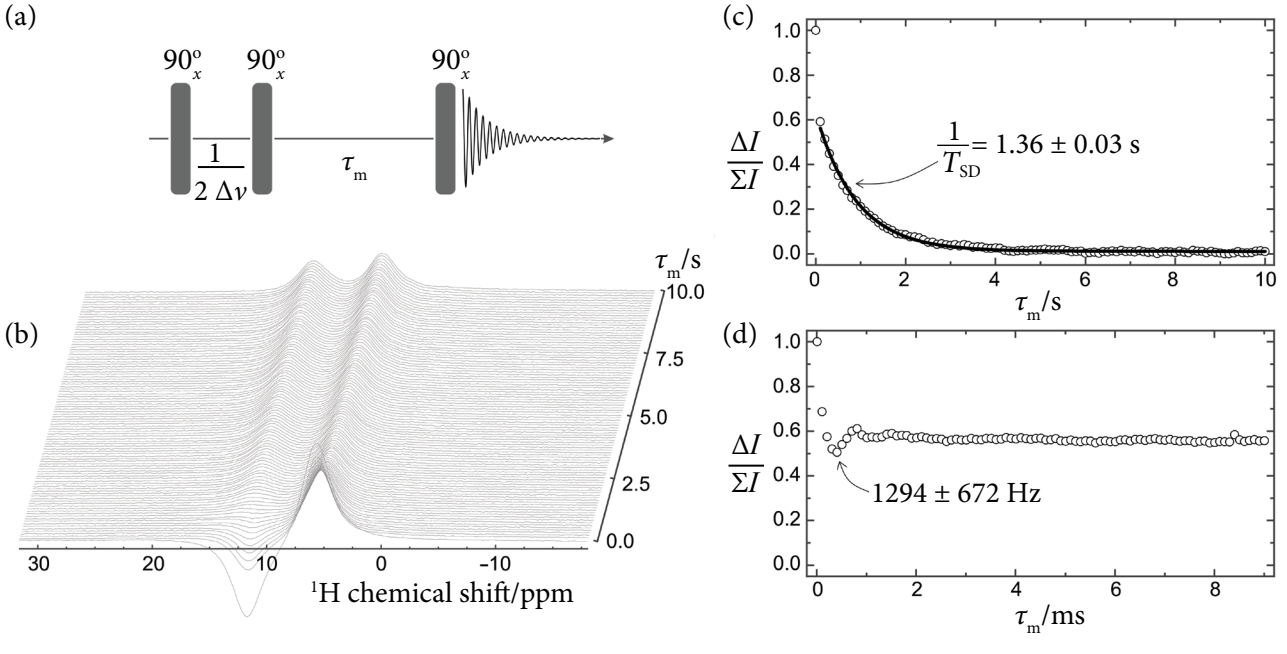

Fig. 3. ^{1}H spin diffusion measurements using (a) the Goldman–Shen pulse sequence consisting of three 90° pulses. The first period with $\Delta\nu$ being resonance difference between two ^{1}H sites, ensures magnetization inversion. (b) The spectra are recorded as a function of the mixing time τ_m. (c) The data is plotted as the relative difference in integral intensity against mixing time τ_m. Here $\Delta I = I_{CH} - I_{COOH}$ and $\Sigma I = |I_{CH}| + |I_{COOH}|$. The black curve represents an exponential fit excluding the first point to estimate the spin diffusion rate. (d) At short mixing times, oscillatory behaviour occurs with the approximate frequency indicated. All experiments were performed under MAS at the rate of 14 kHz.

dipole–dipole coupling by more than a factor of three, the dipolar interaction network as well as chemical shift anisotropy (CSA) become effectively quenched and the system approaches a single-crystal limit.

This interpretation is further supported by the short-mixing-time dynamics shown in Fig. 3(d). The differential intensity $\Delta I/\Sigma I$ exhibits a rapid oscillatory decay within the first millisecond, stabilizing at a plateau corresponding to approximately 55% of the initial value. The central frequency of this oscillation is about 1300 Hz. The oscillatory spin-diffusion behaviour of this kind has been extensively studied in polymers as a function of MAS rate [14–17]. According to the three-spin model, besides the MAS rate, the oscillation frequency is primarily governed by multiple dipole–dipole couplings, in the current case between a carboxylic proton site and two alkene proton sites with internuclear distances of 3.32 and 3.78 Å (see the molecular structure in Fig. 1) [29]. Using the relation $b_{\mathrm{eff}}^2 = b_{12}^2 + b_{13}^2$, the effective coupling is estimated to be approximately 4 kHz. The measured value of 1.3 kHz thus corresponds to MAS averaging of 0.32, slightly higher than the predicted value of 0.22 reported in Fig. 6(b) of Ref. [14]. This discrepancy may stem from experimental uncertainties or from simplifying assumptions for the current structure.

4. Results at varied temperatures

The dynamical properties of ^{1}H spin diffusion were studied at varied temperatures. As seen in Fig. 4, the rate of spin diffusion rapidly accelerates with temperature from 1.36 to 5.35 s^{-1} in just 40 K. This indicates a considerable thermal activation energy, which was estimated to be 28.4 kJ/(mol·K) according to the Arrhenius plot.

Such a steep temperature dependence is not observed in the longitudinal relaxation data. The ^{1}H relaxation times (T_1) increase only slightly from 168 to 193 s for the alkene protons and from 178 to 195 s for the carboxylic protons. Similarly, the ^{13}C relaxation times remain nearly constant, with $T_1 \approx 400$ s for the carboxylic carbon and $T_1 \approx 1030$ s for the alkene carbon. The relatively faster relaxation of the carboxylic carbon likely reflects its larger chemical-shift anisotropy, whereas the overall flat T_1 profiles suggest a regime well outside the extreme-narrowing limit.

The ^{1}H relaxation data further indicate that the correlation time associated with the dominant relaxation mechanism is shorter than the inverse Larmor frequency, despite the rigidity of the molecular framework. Previous studies have shown that, due to the rapid proton exchange within carboxylic acid dimers, the narrowing condition can only be reached well below 200 K [30, 31]. This

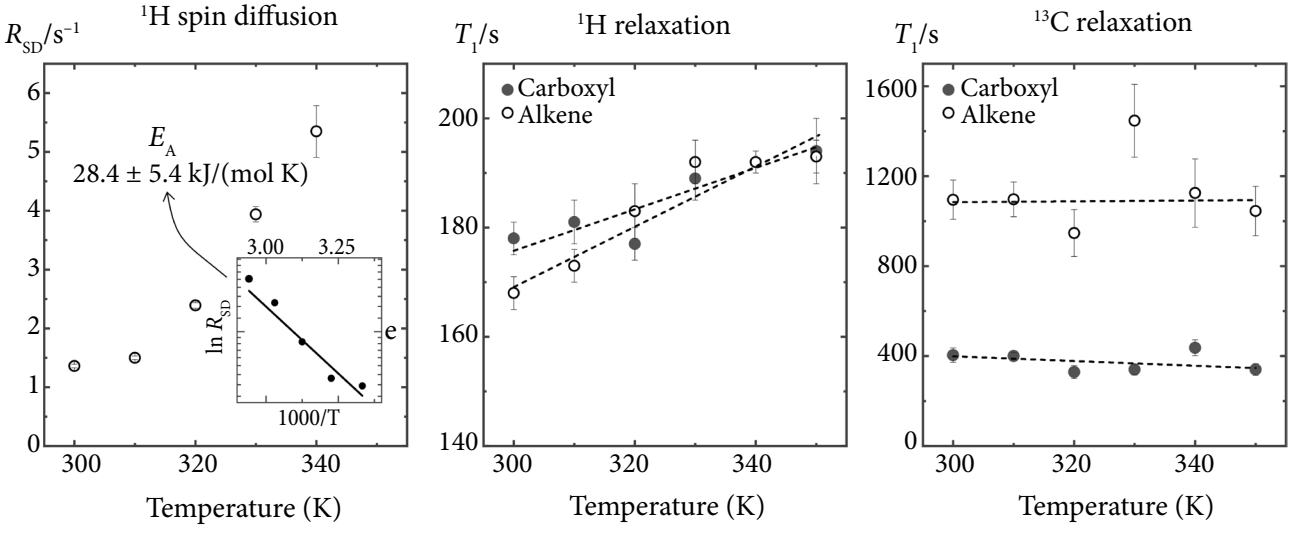

Fig. 4. ^{1}H spin diffusion rates (left), ^{1}H T_1 relaxation times (middle) and ^{13}C T_1 relaxation times (right) measured at different temperatures. A small inset (left) shows the spin diffusion data plotted in the Arrhenius diagram with the best linear fit line shown in black. The calculated thermal activation energy is written above. The linear fit of the relaxation data points is shown as dashed lines and given as a guide. More experimental details are given in the text. Fitting errors using exponential decay functions are given as error bars.

behaviour supports the notion that proton exchange processes continue to influence relaxation dynamics even in the rigid solid structure.

5. Conclusions

In this study, dry powdered fumaric acid was investigated using conventional solid-state NMR techniques. The results reveal that, although the internuclear framework remains highly rigid, the ^{1}H nuclei form a relatively weak dipolar network that gives rise to a slow spin diffusion. Remarkably, increasing the crystal temperature by only 40 K accelerates the ^{1}H spin-diffusion rate by nearly a factor of four. This thermal enhancement is accompanied by an increase in the ^{1}H longitudinal relaxation time T_1 of approximately 20 s, likely arising from proton exchange between carboxylic groups. Overall, these findings provide a new insight into temperature-driven spin-diffusion dynamics in molecular solids and highlight pathways for optimizing polarization transfer in future NMR experiments.

Acknowledgement

With great pleasure, I would like to thank my PhD supervisor prof. Vytautas Balevičius for introducing me to the field of NMR, encouraging independent thinking and displaying a heart-warming generosity towards others. We strive to carry these values forward as the foundation of our future.

References

[1] H.W. Meyer, H. Schneider, and K. Saalwächter, Proton NMR spin-diffusion studies of PS-PB block copolymers at low field: Two- vs three-phase model and recalibration of spin-diffusion coefficients, Polym. J. **44**(8), 748 (2012).

[2] M. Mauri, Y. Thomann, H. Schneider, and K. Saalwächter, Spin-diffusion NMR at low field for the study of multiphase solids, Solid State Nucl. Magn. Reson. **34**(1), 125 (2008).

[3] B. Elena, G. Pintacuda, N. Mifsud, and L. Emsley, Molecular structure determination in powders by NMR crystallography from proton spin diffusion, J. Am. Chem. Soc. **128**(29), 9555 (2006).

[4] T. Manolikas, T. Herrmann, and B.H. Meier, Protein structure determination from ^{13}C spin-diffusion solid-state NMR spectroscopy, J. Am. Chem. Soc. **130**(12), 3959 (2008).

[5] A. Kubo and C.A. McDowell, Spectral spin diffusion in polycrystalline solids under magic-angle spinning, J. Chem. Soc. Faraday Trans. **84**(11), 3713 (1988).

[6] P. Heitjans, S. Indris, and M. Wilkening, Solid-state diffusion and NMR, Diffusion Fundam. **2**, 1 (2005).

[7] D. Suter and R.R. Ernst, Spin diffusion in resolved solid-state NMR spectra, Phys. Rev. B. **32**(9), 5608 (1985).

[8] Y. Matsuki, T. Idehara, J. Fukazawa, and T. Fujiwara, Advanced instrumentation for DNP-enhanced MAS NMR for higher magnetic fields and lower temperatures, J. Magn. Reson. **264**, 107 (2016).

[9] I.B. Moroz, D. Jardón-Álvarez and M. Leskes, The role of spin diffusion in endogenous metal ions DNP, J. Chem. Phys. **162**(2), 024201 (2025).

[10] M. de Oliveira, K. Herr, M. Brodrecht, N.B. Haro-Mares, T. Wissel, V. Klimavicius, H. Breitzke, T. Gutmann, and G. Buntkowsky, Solvent-free dynamic nuclear polarization enhancements in organically modified mesoporous silica, Phys. Chem. Chem. Phys. **23**(22), 12559 (2021).

[11] M. Gierse, L. Dagys, M. Keim, S. Lucas, F. Josten, M.B. Plenio, I. Schwartz, S. Knecht, and J. Eills, Hyperpolarizing small molecules using parahydrogen and solid-state spin diffusion, Angew. Chem. Int. Ed. **63**(34), e202319341 (2024).

[12] M. Goldman and L. Shen, Spin-spin relaxation in LaF_3, Phys. Rev. **144**(1), 321 (1966).

[13] A.M. Kenwright and K.J. Packer, On T_1 cancellation schemes in Goldman–Shen-type experiments, Chem. Phys. Lett. **173**(5), 471 (1990).

[14] M. Roos, P. Micke, K. Saalwächter, and G. Hempel, Moderate MAS enhances local ^{1}H spin exchange and spin diffusion, J. Magn. Reson. **260**, 28 (2015).

[15] K. Schäler, M. Roos, P. Micke, Y. Golitsyn, A. Seidlitz, T. Thurn-Albrecht, H. Schneider, G. Hempel, and K. Saalwächter, Basic principles of static proton low-resolution spin diffusion

NMR in nanophase-separated materials with mobility contrast, Solid State Nucl. Magn. Reson. **72**, 50 (2015).

[16] Q. Chen and K. Schmidt-Rohr, Measurement of the local ^{1}H spin-diffusion coefficient in polymers, Solid State Nucl. Magn. Reson. **29**(1), 142 (2006).

[17] Z. Jia, L. Zhang, Q. Chen, and E.W. Hansen, Proton spin diffusion in polyethylene as a function of magic-angle spinning rate. A phenomenological approach, J. Phys. Chem. A **112**(6), 1228 (2008).

[18] L. Dagys, V. Klimavicius, and V. Balevicius, Processing of CP MAS kinetics: Towards NMR crystallography for complex solids, J. Chem. Phys. **145**(11), 114202 (2016).

[19] L. Dagys, V. Klimkevičius, V. Klimavicius, K. Aidas, R. Makuška, and V. Balevicius, CP MAS kinetics in soft matter: Spin diffusion, local disorder and thermal equilibration in poly(2-hydroxyethyl methacrylate), Solid State Nucl. Magn. Reson. **105**, 101641 (2020).

[20] L. Dagys, V. Klimavicius, M. Brodrecht, G. Buntkowsky, and V. Balevicius, Cross-polarization kinetics and fractal nature of thermal equilibration in spin systems: From low-dimensional proton conductors to tripeptides, J. Phys. Chem. Solids **152**, 109946 (2021).

[21] D.H. Brouwer and J.A. Ripmeester, Symmetry-based recoupling of proton chemical shift anisotropies in ultrahigh-field solid-state NMR, J. Magn. Reson. **185**(1), 173 (2007).

[22] H.K. Miah, R. Cresswell, D. Iuga, and J.J. Titman, ^{1}H CSA parameters by ultrafast MAS NMR: Measurement and applications to structure refinement, Solid State Nucl. Magn. Reson. **87**, 67 (2017).

[23] M.H. Levitt, D. Suter, and R.R. Ernst, Spin dynamics and thermodynamics in solid-state NMR cross polarization, J. Chem. Phys. **84**(8), 4243 (1986).

[24] C.A. Fyfe, A.R. Lewis, and J.-M. Chézeau, A comparison of NMR distance determinations in the solid state by cross polarization, REDOR, and TEDOR techniques, Can. J. Chem. **77**(11), 1984 (1999).

[25] K.T. Mueller, Analytic solutions for the time evolution of dipolar-dephasing NMR signals, J. Magn. Reson. A. **113**(1), 81 (1995).

[26] F. Vogt, D. Aurentz, and K. Mueller, Determination of internuclear distances from solid-state nuclear magnetic resonance: Dipolar transforms and regularization methods, Mol. Phys. **95**(5), 907 (1998).

[27] J. Lorieau and A.E. McDermott, Order parameters based on $^{13}C^{1}H$, $^{13}C^{1}H_{2}$ and $^{13}C^{1}H_{3}$ heteronuclear dipolar powder patterns: A comparison of MAS-based solid-state NMR sequences, Magn. Reson. Chem. **44**(3), 334 (2006).

[28] M. Wang, M. Bertmer, D.E. Demco, and B. Blümich, Segmental and local chain mobilities in elastomers by ^{13}C– ^{1}H residual heteronuclear dipolar couplings, J. Phys. Chem. B. **108**(30), 10911 (2004).

[29] A.O.L. Évora, D.F. Valente-Matias, C.E.S. Bernardes, C.M. Lousada, M.F.M. Piedade, M. Lusi, H.P. Diogo, and M.E. Minas da Piedade, Structure, cohesion energetics, and hydrogen bonding cooperativity in fumaric acid and alkyl fumarates: Insights from experiment and theory, Crys. Growth Des. **24**(22), 9465 (2024).

[30] B.H. Meier, F. Graf, and R.R. Ernst, Structure and dynamics of intramolecular hydrogen bonds in carboxylic acid dimers: A solid state NMR study, J. Chem. Phys. **76**(2), 767 (1982).

[31] S. Nagaoka, T. Terao, F. Imashiro, A. Saika, N. Hirota, and S. Hayashi, An NMR relaxation study on the proton transfer in the hydrogen bonded carboxylic acid dimers, J. Chem. Phys. **79**(10), 4694 (1983).

APIE PROTONŲ SUKINIO DIFUZIJĄ MILTELIŲ PAVIDALO FUMARO RŪGŠTYJE

L. Dagys

Vilniaus universiteto Fizikos fakulteto Cheminės fizikos institutas, Vilnius, Lietuva

Santrauka

Sukinio difuzija yra plačiai paplitęs reiškinys kietojo kūno branduolinio magnetinio rezonanso (BMR) srityje, leidžiantis tirti molekulinę struktūrą ir pernešti magnetizaciją dideliais tarpmolekuliniais atstumais. Neseniai parodėme, kad stipriai poliarizuotų ^{13}C branduolių poliarizacija gali būti perduodama netgi tarp atskirų kristalitų, pradedant nuo hiperpoliarizuotos 1-^{13}C-fumaro rūgšties. Šiame darbe sausa miltelių pavidalo fumaro rūgštis buvo tiriama taikant įprastinius kietojo kūno BMR metodus, siekiant charakterizuoti sukinių difuzijos savybes tankiame ^{1}H branduolių tinkle. Rezultatai rodo, kad nors sukinio difuzija šioje rūgštyje yra lėta, jos greitis ir poliarizacijos gyvavimo trukmė didėja kylant temperatūrai. Šie duomenys suteikia naujų įžvalgų apie protonų nulemtą sukinių difuzijos mechanizmą ir gali būti svarbūs kuriant efektyvesnes poliarizacijos perdavimo strategijas.